CHEMICAL ENGINEERING TRANSACTIONS
VOL. 86, 2021
A publication of AIDIC
The Italian Association of Chemical Engineering
Online at www.cetjournal.it
Guest Editors: Sauro Pierucci, Jiří Jaromír Klemeš

ISBN 978-88-95608-84-6; **ISSN** 2283-9216

Towards Real-Time Control of a Semibatch Crystallization Process by Electrical and Ultrasound Tomographic Techniques

Soheil Aghajanian[a,*], Guruprasad Rao[b], Panagiotis Koulountzios[c], Lidia Jackowska-Strumillo[b], Manuchehr Soleimani[c], Tuomas Koiranen[a]

[a]Department of Separation Science, LUT University, Yliopistonkatu 34, P.O. Box 20, FI-53851 Lappeenranta, Finland
[b]Institute of Applied Computer Science, Lodz University of Technology, Ulica Stefanowskiego 18/22, 90/924 Lodz, Poland
[c]Engineering Tomography Laboratory (ETL), Department of Electronic and Electrical Engineering, University of Bath, Claverton Down, BA2 7AY, UK
soheil.aghajanian@lut.fi

This research work presents a feasibility study to demonstrate the application of Electrical Resistance Tomography and transmission-based Ultrasound Computed Tomography for monitoring and control of micron-sized calcium carbonate crystallization process. Herein, precipitated calcium carbonate production is bind to a carbon dioxide absorption process based on hollow-fiber membrane contactor.
ERT acquisition system is equipped with 16 electrodes with operating frequency of 156 KHz and image capturing frame rate of 2 Hz. The ultrasound tomography equipment consists of 32 piezoelectric transducers at a frequency of 200 KHz. These sensors are sensitive to changes in suspension density and conductivity. Furthermore, a process control framework is developed by utilizing the fundamental relations of settling velocity of particles. Through simulations in the LabVIEW software, the PI-based feedback controller demonstrates a possibility of setpoint tracking by manipulating the control variable (mixing speed). Upon further investigations, this approach can be used as a multi-dimensional process analytical technology tool for quality assurance and malfunction diagnosis when out-of-specification events occur throughout the entire process.

1. Introduction

Crystallization technique combines both particle formation and purification, which makes it vital to many processes, and is regarded as the most significant unit operation worldwide. The proposed crystallization application of this study is micron-sized precipitated calcium carbonate, which has extensive applications in different industries such as: soft glasses (Almer, 2017), filler material in papers and plastics (Gao et al., 2018). Of particular interest, is reaction type crystallization (reactive crystallization, precipitation); the behavior of precipitation systems is determined by interaction of multiple process phenomena such as nucleation, growth, spatial and temporal distribution of species concentration through mixing and addition rate of the reagent to the crystallizer. Crystallization process monitoring and real-time evaluation are considered as key operations that not only affect the characteristics of the post-filtration product, but also could facilitate the routes toward lowering the energy and raw material consumption. Hence, applications of novel in-situ monitoring and sensor technologies, imaging modalities and algorithms are always required to control and monitor such processes.
In recent years, and following the process analytical technology concept, several spectroscopy-based sensing instruments have been developed for crystallization process monitoring (Yang et al., 2015). Owing to recent advances in sensor technologies and computational power, tomographic sensors have shown great potential to be used in crystallization processes. These tomographic sensors with their reconstruction algorithms can provide significant amount of data from internal characteristics of the process, which can be exploited for further visualization and quantification. Unlike spectroscopic methods, tomographic measurements could provide a

framework to obtain spatio-temporal information about a process. Such tomography-based measurements, which are the focus of the present study, are different variants of electrical tomography and new emerging ultrasound computed tomography.
The application of electrical resistance tomography (ERT) for crystallization is still in early research phase. Most of the works using tomographic techniques have been focused on monitoring the extent of mixing and homogeneity analysis (Sharifi and Young, 2013). Investigation of ERT for development of active pharmaceutical ingredients during a cooling crystallization has also been demonstrated (Ricard et al., 2005). On the other hand, applicability of ultrasound computed tomography (USCT) in crystallization is seldom reported. Given that measurement techniques based on ultrasonic wave propagation have a potential for non-invasive and non-intrusive operation, it can be utilized for online monitoring of crystallization processes (Koulountzios et al., 2019). The purpose of the present contribution is to develop a mathematical framework and process control scheme to integrate and transform ERT- and USCT-based monitoring signals as an input for a PI (proportional–Integral) controller during a micron-sized calcium carbonate precipitation process. The mathematics are based on fundamental relations of fluid mechanics and settling velocity of particles in suspension, which are implemented in the LabVIEW software environment. Being entirely a multidisciplinary and joint research work, improvement of the methodology under investigation progressively increases.

2. Materials and methods

2.1 Integrated crystallization and CO_2 capture process description

In the present work, crystallization system that results in micron-sized calcium carbonate is integrated with a carbon dioxide (CO_2) absorption process. The adapted approach for production of calcium carbonate ($CaCO_3$) by binding it to a CO_2 capture process can be considered as a potential post–combustion technology for carbon capture, utilization and sequestration (CCUS), in which high energy heat consumption for CO_2 desorption is avoided by manufacturing a high added-value chemical. This can also be beneficial in circular economy processes using waste materials.
Integration of these separation methods is based on the idea of high absorption rate of CO_2 gas in strong OH^--based solutions and the chemical reaction that enables the dominance of CO_3^{2-} formation in highly alkaline conditions. In the present process, different concentrations of aqueous NaOH (VWR, Purity > 99.1 %) were used as absorption solution to perform the CO_2 capture process. Experimental setup consists of an in-house carbon capture unit based on hollow fiber membrane contactor (Liqui-Cel Extra-Flow, 3M) (Nieminen et al., 2020) and a stainless-steel crystallizer of diameter 200 mm (Height/Diameter = 1.6) equipped with an overhead stirrer (Heidolph Instruments). In the membrane module, the liquid and gas phases are circulated on a countercurrent flow pattern; the gas stream flows downwards on the shell side of the membrane, while the absorbent liquid flows countercurrent into the hollow fibers. Thus, precise pressure measurement control across the membrane module is critical to prevent phase dispersion. Herein, the pressure at the gas outlet of the membrane was maintained at 0.1 bar below the incoming liquid inlet pressure.
The semibatch feed contains dissociated CO_3^{2-}, OH^- and Na^+ ionic solution at a pH level below the calcium hydroxide ($Ca(OH)_2$) solubility at 20 °C (pH = 12.37). Operating below the $Ca(OH)_2$ solubility, limits its formation during the process. Given the three–order of magnitude difference between solubility product of $CaCO_3$ (K_{sp} = 3.36 × 10^{-9} at 25 °C) and $Ca(OH)_2$ (K_{sp} = 5.5 × 10^{-6} at 25 °C), crystallization of the latter component can be avoided (Moffitt Schall and Myerson, 2019).
Therefore, post–absorption CO_2–rich solvents were used to carry out a crystallization process instead of heating the sodium carbonate and sodium bicarbonate solutions for releasing the CO_2 gas via a caustic recovery at 800 °C 109.4 kJ mol^{-1} CO_2. The pH-controlled crystallization is favorable in atmospheric pressure and ambient temperature (20 ± 2 °C) and occurs by addition of the feed solution (through a 2-mm pipe) to a reactor containing calcium chloride (Anhydrous, Merck ≥ 98 %) according to the chemical reaction Eq(1).

$$CO_3^{2-}{}_{(aq)} + 2\ Na^+{}_{(aq)} + CaCl_{2\,(aq)} \rightarrow CaCO_{3\,(s)} \downarrow + 2\ NaCl_{(aq)} \quad (1)$$

Volume mean particle diameter (D_{43}) of the final product from each crystallization operation was evaluated by laser diffraction method in a particle size analyzer Mastersizer 3000 (Malvern Instruments), and total CO_2 content ($mol\ L^{-1}$) of the rich solvent was determined by a titration technique using Chittick apparatus (Soham Scientific). Figure 1 shows the overall schematic of the entire process.

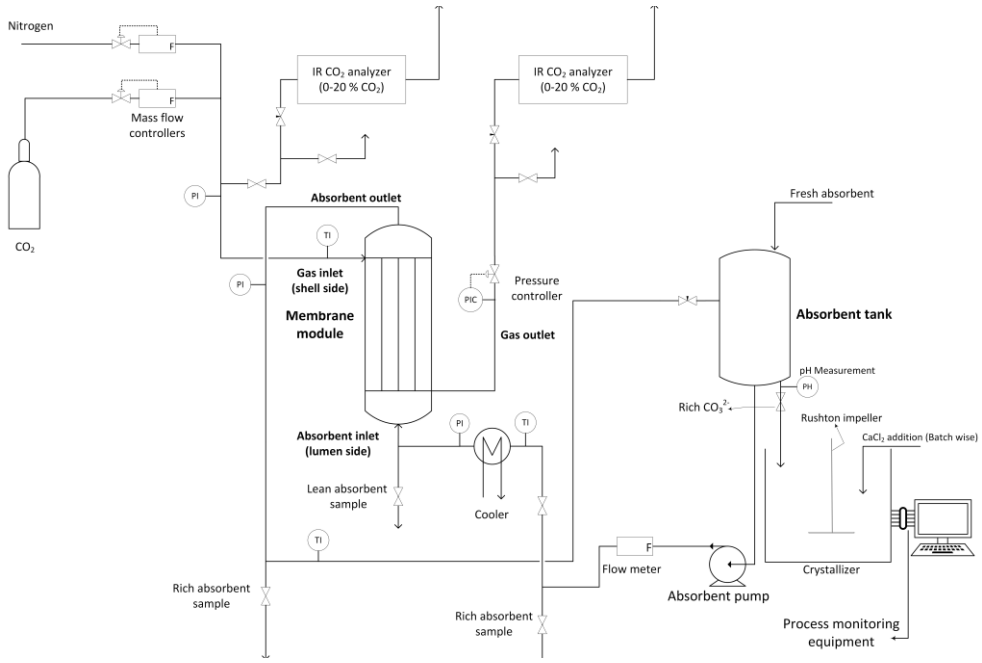

Figure 1: Schematic of the integrated carbon dioxide capture and calcium carbonate crystallization setup with process monitoring equipment (tomographic sensors).

2.2 Electrical resistance tomography

Electrical resistance tomography is a technique of electrical voltage or current injection and measuring the electrical field distribution to reconstruct a three-dimensional image using inverse imaging methods. These reconstructed images provide conductivity distribution in a planar view of the circular sensor and could be proportional to solid particle formation in the planar region of interest. Therefore, the rector was equipped with a single row of 16 electrodes mounted around the perimeter; a constant voltage is injected though one electrode and electrical current is measured simultaneously using the remaining 15 electrodes. The frequency of operation is 156 KHz and image capturing frame rate is 2 Hz. A modified Bayesian method is utilized for image reconstruction (Rao et al., 2020).

2.3 Ultrasound computed tomography

The proposed ultrasound computed tomography system can be divided into three basic components: an array of multi-piezoelectric sensors, a sensing electronics setup for data acquisition and a computer system for image reconstruction. This system consists of a ring of 32 piezoelectric transducers operating at a frequency of 200 KHz. The most commonly used approximation for USCT is the ray-based method; it is the fundamental foundation for the most tomographic schemes. The main advantage is the computational efficiency due to the fact that the continuous wave equation is solved using finite number of rays, which describe the wave propagation. In the case of a uniform sound speed model that only depends on the depth, a convenient parameterization for the rays can be used. To avoid the drawbacks and limitations of the straight-ray model in USCT data acquisition, an alternate approach of ultrasound transmission tomography's sensitivity kernels is adopted. This method is created by thickening the straight lines and then smoothening them along their direction using a standard deviation. A sensitivity matrix of smoothed lines with an angle beam of 90-degree is used due to higher accuracy.

2.4 Process control simulation procedure

Values of resistance and transmission varies due to change in suspension density and settlement of particles at different heights along the crystallizer. Multiple layers of sensors mounted around the reactor could measure changes in characteristics of the medium through 1-D point-to-point conductivity or sound speed evaluations. These measurements, which will be correlated to particle settling velocity, thus can be used as input signal for process control system. In Newtonian fluids, particle settling velocity is a function of solid particle concentration; it decreases as suspension density increases within the fluid domain. The free settling velocity of spherical particles, V_t, with an average size ranging from 3 to 10 microns and particle Reynolds number between 0.0001 and 0.3, is defined based on Stokes' law (Atiemo-Obeng et al., 2004):

$$d_p = \left(\frac{18\, V_t\, \mu}{g(\rho_s - \rho_f)}\right)^{1/2} \quad (2)$$

Where, ρ_f and ρ_s are fluid and solid density, respectively; d_p represents particle diameter, g is gravitational acceleration and μ denotes the dynamic viscosity of the fluid. Free settling velocity is suitable to employ in low solid volume fractions, ϕ (Koo, 2009). For the current feasibility demonstration, suspension density is maintained below 0.05 % and process simulations are conducted based on this assumption. Measuring particle settlement requires switching on/off the stirrer and feed flow. Tomographic signals obtained at different heights of the reactor could be an indicator of settlement of particles; based on the vertical distance between the sensors and time of the measurements, settling velocity could be approximated, which in turn results in the calculation of average diameter. Signal acquisition, conversion and scaling is a critical phase for real case implementation and is under investigation.

The above-mentioned scenario is implemented in the LabVIEW (National Instruments) software, and a variable step response signal (i.e., settling velocity) is used as an input to the system; thus, average particle diameter is evaluated based on Eq(2) and then stored in a buffer layer (temporary data storage). Eventually, the calculated size is averaged over a specific sample length in order to have a reasonable approximation of the transient distribution of particle size. In case of a difference between the setpoint diameter of the controller and calculated value from the input signal, a traditional PI controller applies the appropriate corrective actions on the manipulated variable (mixing speed) within the next operational loop of the process.

3. Results and discussion

3.1 Effect of operating conditions on crystallization process

Changes in operating conditions (e.g., mixing, feed rate) directly impacts the mixing–sensitive liquid-liquid crystallization reaction by affecting the mass transfer and diffusion rate, and particle growth phenomena. In this work, addition of 0.1 L of the feed solution to the receiving reactor containing 2 L of calcium chloride-water solution conducted at a constant rate of 2 ml/min at three different mixing speeds of 50, 150 and 250 RPM. calcium chloride was used in excess amount with an initial concentration of 0.013 mol/L. Additionally, only one post-capture CO_2–loaded solution with initial absorbent concentration of 2.24 ± 0.04 mol/L were used. Table 1 presents the combined results of CO_2 absorption and the crystallization process. It shows that an increase in mixing speed at a constant feed addition rate, monotonically increases $CaCO_3$ particle size. At higher mixing rates, reagent distribution becomes comparatively faster, which in turn limits the excessive nucleation; this phenomenon favors particle growth in the crystallizer.

Table 1: $CaCO_3$ particle size diameter at three mixing speeds of 50, 150 and 250 RPM at a constant feed addition rate of 2 ml/min; obtained with initial absorbent solution concentration of 2.24 ± 0.04 mol/L.

Initial absorbent concentration, [mol/L]	Total CO_2 content (post-capture), [mol/L]	Mixing speed, [RPM]	Residence time, [min]	Precipitation yield, [%]	Suspension density (ϕ), [vol-%]	Average volumetric size, [µm]
2.24 ± 0.04	0.13 ± 0.05	50	50	89	0.003	5.4 ± 0.4
		150	50	94	0.01	8.6 ± 0.6
		250	50	91	0.02	10.7 ± 0.5

3.2 Tomographic measurements

Preliminary tomographic measurements with USCT are carried out with different concentrations of small-sized solid particles in water solutions at 20 °C. The developed measurement techniques are demonstrated to be sensitive to concentration variations and subsequently to density. Figure 2a shows the acquired results by utilizing sound-speed imaging based on transmission ultrasound tomography method, where it responds accurately to the slight changes in concentration of the slurry mixtures. The results follow an ascending trend as the solid particle concentration increases in the binary mixture. Additionally, Figure 2b and 2c display tomographic reconstruction of a mixture with low concentration by using Total Variation regularization method and schematic illustration of the USCT system, respectively.

Alongside ultrasound tomography, a 2D-ERT technique has been implemented to monitor the conductivity distribution during calcium carbonate precipitation. In this study, initial experiments with ERT are carried out at a lower suspension density of 0.1–0.25 vol-%, allowing a more precise calculation of conductivity in the ionic solution. It is expected that more accurate operation at higher suspension densities can be made possible by

further development of the monitoring unit. Figure 3a shows reconstructed images of a 10 mm diameter non-conductive phantom in water. Figure 3b displays a relative conductivity distribution at the vertical mid-section of the reactor during initial stages of the process; these reconstructions correspond to density distribution in the ionic medium.

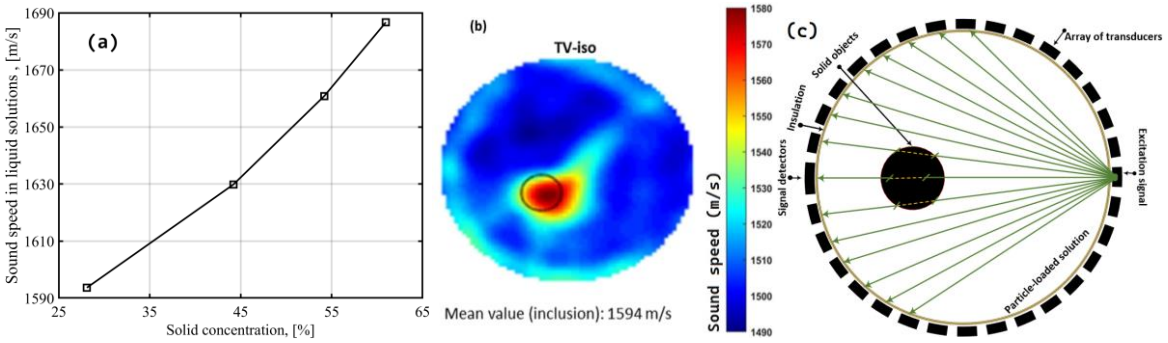

Figure 2: (a) Sound-speed results of the slurries from four experiments using different particle concentrations; (b) A Total Variation reconstruction; (c) Schematic illustration of the developed USCT system.

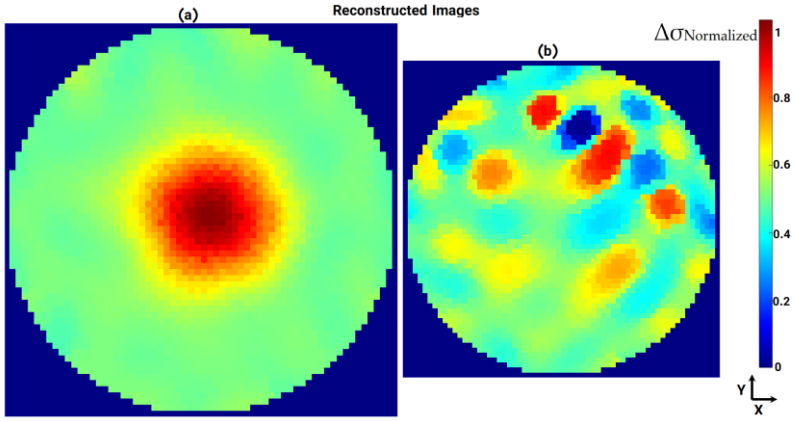

Figure 3: Characterization of solution composition by ERT; (a) Reconstruction of a 10 mm diameter phantom; (b) Normalized cross sectional view of ERT measurements at the vertical mid-section of the reactor.

3.3 Controller simulation

To carry out the process simulation by manipulating the control variable and to determine the approximate process output (mean size), a step function corresponding to free terminal velocity signal is introduced. The controller is developed to maintain the particle diameter on a predefined value based on setpoint tracking approach. Figure 4 shows the results obtained from step interrogation of the process model.

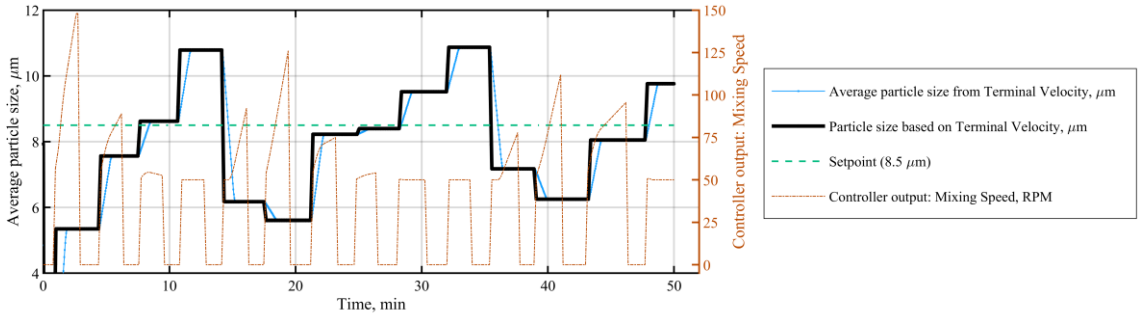

Figure 4: PI controller response for setpoint tracking within the operational bounds of the experiments; variation in manipulated variable (mixing speed) during the simulation.

The logic behind the PI controller is according to average volumetric size reported in Table 1 in which particle size increases by a rise in mixing speed and vice versa. Current value of the output parameter is calculated through the input signal to the process algorithm, and then fed back to the controller; the difference between the setpoint and measured output is determined and in case of difference, an actuating signal is generated by the PI controller. Actuating signal adjusts the mixing rate, which is subjected to constrains between 50 – 150 RPM, in a manner that it increases when particles are below the setpoint. The rate of change in the mixing speed is controlled in real-time by the gain parameters of the PI controller, K_p and K_i. Herein, values of K_i is changed between 0.35 – 0.45, while K_p is constant at 0.05. Values of K_i and K_p are obtained by trial and error. Since the estimated values lead to a desirable behavior for the process under investigation, a thorough tuning process is neglected.

4. Conclusions

In conclusion, this feasibility study demonstrates an approach to integrate a CO_2 capture technique, its utilization for manufacturing micron-sized calcium carbonate and use of tomographic techniques for process control and quality assurance. Through experiments with an in-house carbon capture unit, it has been shown that 0.13 ± 0.05 mol/L CO_2 can be absorbed in OH^--rich absorbent solution with concentration of 2.24 ± 0.04 mol/L; upon adjusting solution pH, the CO_2-loaded solution can be used to manufacture micron-sized (5–11 µm) $CaCO_3$.
The developed ERT and sound-speed tomography equipment proved to be capable of online monitoring of variations in characteristics of the medium based on conductivity and density and can be utilized to perform a multi-dimensional quantitative analysis of a crystallization processes. Moreover, a PI-based controller scheme is proposed and simulated by coupling the free settling velocity formulation of Stokes' Law to the process model. It has been shown that actuating signal generated by the PI controller can adjust the manipulated variable according to a given setpoint. Integrating the actual tomographic signal to the process control scheme and improving the robustness of the operational procedures are among the key objectives of future works.

Acknowledgments

This project has received funding from the European Union's Horizon 2020 research and innovation programme under the Marie Skłodowska-Curie Grant Agreement No. 764902.

References

Almer, J., 2017. Engineering materials, in: Synchrotron Radiation News. Cambridge University Press, pp. 2–3. https://doi.org/10.1080/08940886.2017.1316123

Atiemo-Obeng, V.A., Penney, W.R., Armenante, P., 2004. Solid–Liquid mixing, in: Handbook of Industrial Mixing. John Wiley & Sons, Inc., Hoboken, NJ, USA, pp. 543–584. https://doi.org/10.1002/0471451452.ch10

Gao, S., Liu, J., Gao, G., 2018. Experimental study on structure and property of chemical building materials based on SEM analysis technology. Chem. Eng. Trans. 66, 1135–1140. https://doi.org/10.3303/CET1866190

Koo, S., 2009. Estimation of hindered settling velocity of suspensions. J. Ind. Eng. Chem. 15, 45–49. https://doi.org/10.1016/j.jiec.2008.08.013

Koulountzios, P., Rymarczyk, T., Soleimani, M., 2019. A Quantitative ultrasonic travel-time tomography to investigate liquid elaborations in industrial processes. Sensors 19, 5117. https://doi.org/10.3390/s19235117

Moffitt Schall, J., Myerson, A.S., 2019. Solutions and solution properties, in: Handbook of Industrial Crystallization. Cambridge University Press, pp. 1–31. https://doi.org/10.1017/9781139026949.001

Nieminen, H., Järvinen, L., Ruuskanen, V., Laari, A., Koiranen, T., Ahola, J., 2020. Insights into a membrane contactor based demonstration unit for CO2 capture. Sep. Purif. Technol. 231, 115951. https://doi.org/10.1016/j.seppur.2019.115951

Rao, G., Aghajanian, S., Koiranen, T., Wajman, R., Jackowska-Strumiłło, L., 2020. Process monitoring of antisolvent based crystallization in low conductivity solutions using electrical impedance spectroscopy and 2-D electrical resistance tomography. Appl. Sci. 10, 3903. https://doi.org/10.3390/app10113903

Ricard, F., Brechtelsbauer, C., Xu, X.Y., Lawrence, C.J., 2005. Monitoring of Multiphase Pharmaceutical Processes Using Electrical Resistance Tomography. Chem. Eng. Res. Des. 83, 794–805. https://doi.org/10.1205/cherd.04324

Sharifi, M., Young, B., 2013. Electrical Resistance Tomography (ERT) applications to Chemical Engineering. Chem. Eng. Res. Des. 91, 1625–1645. https://doi.org/10.1016/j.cherd.2013.05.026

Yang, Y., Song, L., Nagy, Z.K., 2015. Automated direct nucleation control in continuous mixed suspension mixed product removal cooling crystallization. Cryst. Growth Des. 15, 5839–5848. https://doi.org/10.1021/acs.cgd.5b01219